Journal of Membrane Science 548 (2018) 694–701

Contents lists available at ScienceDirect

Journal of Membrane Science

journal homepage: www.elsevier.com/locate/memsci

Elucidating the mechanisms underlying the difference between chloride and nitrate rejection in nanofiltration

Razi Epsztein[a], Wei Cheng[a,b], Evyatar Shaulsky[a], Nadir Dizge[a,c], Menachem Elimelech[a,*]

[a] Department of Chemical and Environmental Engineering, Yale University, New Haven, CT 06520-8286, USA
[b] State Key Laboratory of Urban Water Resource and Environment, Harbin Institute of Technology, Harbin 150090, China
[c] Department of Environmental Engineering, Mersin University, Mersin 33343, Turkey

ARTICLE INFO

Keywords:
Nanofiltration
Nitrate rejection
Chloride rejection
Layer-by-layer
Rejection ratio
Activation energy

ABSTRACT

Despite the strong similarity between chloride (Cl^-) and nitrate (NO_3^-) anions in terms of their hydrated radius and charge, Cl^- is rejected more favorably than NO_3^- by nanofiltration (NF) membranes. The main goal of this study is to provide a better understanding of the removal mechanisms favoring the higher rejection of Cl^- over NO_3^- in NF. A series of experiments with polyamide (NF270) and cellulose acetate (CK) NF membranes at different pH values, followed by calculation of the activation energies for Cl^- and NO_3^- passage through the membranes, showed that the higher Cl^- than NO_3^- rejection is attributed to both size-exclusion and Donnan (charge)-exclusion mechanisms. At a neutral membrane charge, a size-exclusion mechanism dominates the rejection of both anions. In this case, we observe higher rejection of Cl^- over NO_3^- due to the lower hydration energy of NO_3^-, which corresponds to higher degree of dehydration and thus higher rate of passage through the NF membrane pores. At a negative membrane charge, the smaller volume of Cl^- compared to NO_3^-, corresponding to higher ionic charge density, results in a stronger electrostatic repulsion of Cl^- by the negatively charged membrane and therefore higher Cl^- rejection than NO_3^-. The coupling of size- and Donnan-exclusion mechanisms with the NF270 membrane results in a maximum Cl^- to NO_3^- rejection ratio at near the isoelectric pH where the membrane is slightly negatively charged. At a positive membrane charge, the sodium (Na^+) counter ions dictate salt rejection independently of the anion type, resulting in almost similar rejections of Cl^- and NO_3^-. Based on the insight gained from these experiments, a layer-by-layer (LbL) polyelectrolyte modification was applied to the NF270 membrane to control its surface charge. This modification showed that shifting the isoelectric point of the NF270 membrane from its original value (pH 4–5) to higher values (pH 6–9) increased the Cl^- to NO_3^- rejection ratio at near neutral pH conditions, thus providing further support for our proposed mechanism underlying the difference between Cl^- and NO_3^- rejection by NF membranes.

1. Introduction

Nanofiltration (NF) is a membrane technology with separation characteristics between reverse osmosis (RO) and ultrafiltration (UF) [1–5]. Salt rejection in NF membranes is based mainly on size (steric)- and Donnan (charge)-exclusion mechanisms [6]. A unique feature of many NF membranes is their high selectivity for the passage of monovalent ions over larger ions and molecules, which is exploited in various applications for removing divalent salts and small organic molecules [3]. However, with respect to rejection of monovalent ions, the selectivity difference is much smaller and the mechanism for such selectivity difference is relatively poorly understood.

Chloride (Cl^-) and nitrate (NO_3^-) are common monovalent anions that are ubiquitous in natural waters and wastewaters. Nitrate is a major pollutant in groundwater and is associated with eutrophication of water bodies [7] and methemoglobinemia, known as the 'blue baby syndrome' [8]. Chloride is the major target anion in desalination processes [9,10] and can be harmful for crops above a certain level [11]. Despite the strong similarity between these two anions, especially in terms of their charge (−1 for both Cl^- and NO_3^-) and hydrated radius (0.33 and 0.34 nm for Cl^- and NO_3^-, respectively) [12,13], higher NF rejection of Cl^- than NO_3^- has been observed in numerous studies [14–20].

A first explanation suggested in several studies [14,15,21] is that NO_3^-, with a larger molar volume, would have a lower ionic charge density compared to Cl^-, which has a smaller molar volume. Thus, the repulsion of NO_3^- by a negatively charged membrane would be weaker and its rejection lower than the rejection of Cl^-. However, this

* Corresponding author.
E-mail address: menachem.elimelech@yale.edu (M. Elimelech).

http://dx.doi.org/10.1016/j.memsci.2017.10.049
Received 14 June 2017; Received in revised form 10 September 2017; Accepted 24 October 2017
Available online 31 October 2017
0376-7388/

explanation, relating the difference between the rejections of the two anions to the Donnan (charge)-exclusion mechanism, was never tested or validated.

Another explanation, associated more with a size-exclusion mechanism, attributed the higher Cl^- rejection to its higher hydration energy (−376 kJ/mol) compared to that of NO_3^- (−329 kJ/mol) [19,22,23]. This explanation is based on a theory suggesting that an ion with a lower hydration energy can strip and rearrange the water shells surrounding it and fit more easily into the membrane pores [24–27]. More recently, Richards et al. [28] used molecular dynamics simulations to show that partial dehydration controls the transport of several anions (including Cl^- and NO_3^-) through NF membranes. However, in a follow-up experimental investigation by the same group [29], the difference between the dehydration degree of Cl^- and NO_3^-, which was evaluated by determining the activation energy for the anion passage through the membrane, was found to be very small and inconsistent for different types of membranes.

Another explanation attributed the higher rejection of Cl^- to the higher degree of hydration of the NO_3^- ion, which reduces its effective surface charge and therefore also its retention [30,31]. However, this explanation is questionable since Cl^- has a higher hydration energy than NO_3^-. A couple of older studies speculated that NO_3^- has higher affinity to the membrane polymer than Cl^- [32,33]. The variety of explanations presented indicates that the reason for the difference in rejection of Cl^- and NO_3^- in NF is still not well understood and emphasizes the need for a more systematic investigation to address this issue.

The main objective of this study is to systematically investigate the mechanisms leading to the difference in rejection of Cl^- and NO_3^- in NF. Specifically, we have studied the effect of membrane charge on the rejection of the two anions by using a charged polyamide NF membrane and an uncharged cellulose acetate NF membrane. We also evaluated the activation energy for the passage of Cl^- and NO_3^- through the two membranes. Our results suggest that both charge- and size-exclusion mechanisms promote higher rejection of Cl^- than NO_3^- and lead to a maximum Cl^- to NO_3^- rejection ratio near the isoelectric pH. The implications of these results for membrane design, to increase the Cl^- to NO_3^- rejection ratio, were evaluated and discussed.

2. Materials and methods

2.1. Materials and chemicals

Two commercial NF membranes were used for the tests: polyamide NF270 (Dow FilmTec) and cellulose acetate CK (GE Osmonics). According to the manufacturers, the NF270 and CK membranes have molecular weight cut-offs of approximately 400 and 2000 Da, respectively. The NF270 membrane was also used as the substrate for membrane modification. Poly (sodium styrene sulfonate) (PSS; MW 70,000 g/mol), poly (diallyl dimethyl ammonium chloride) (PDADMAC; MW 150,000–200,000 g/mol, 20 wt% in water), poly (allyl amine hydrochloride) (PAH; MW 450,000 g/mol), poly (acrylic acid) (PAA; MW 100,000 g/mol), and sodium nitrate ($NaNO_3$) were purchased from Sigma-Aldrich. Sodium chloride (NaCl), isopropanol, and glycerol were purchased from J.T. Baker Chemicals. Hydrochloric acid (HCl) was purchased from AmericanBio, and sodium hydroxide (NaOH) was purchased from Macron Fine Chemicals. Deionized water (MilliPore Academic A-10, resistance 15 MΩ-cm) was used for preparing solutions, compaction of membranes, and rinsing the NF system.

2.2. Nanofiltration system and anion rejection experiments

A bench-scale system operating in cross-flow mode with a flat sheet membrane cell was used for all membrane tests. The total surface area of the membranes tested was 20.02 cm^2. Water was recirculated from the feed tank over the membrane cell with an applied inlet pressure between 3.4 and 5.5 bar (50 and 80 psi) (the specific pressure applied for each experiment is indicated in Section 3) and cross flow velocity of 21.4 cm/s. Before use, the commercial membranes were agitated in 25% isopropanol solution for 30 min using a rotating shaker. Then, the membranes were rinsed with deionized water three times (each time for 30 min) and kept overnight in deionized water to remove impurities. Prior to filtration, all membranes (commercial and modified) were compacted overnight under pressure between 4.8 and 6.9 bar (70–100 psi). Except for the experiments to determine the activation energy for anion transport through the membranes (Section 3.2), water temperature was maintained constant at 25 °C. For the experiments to determine the activation energy, temperature was increased gradually from 25 °C to 40 °C and samples were taken at four different temperatures of 25, 30, 35, and 40 °C. Feed solution pH was monitored and adjusted throughout all experiments using hydrochloric acid or sodium hydroxide. For each membrane test, feed and permeate were collected for Cl^- and NO_3^- analysis by ion chromatography (Dionex DX-500 with an AS14A IonPac column). All experiments were carried out with deionized water amended with NaCl and/or $NaNO_3$.

2.3. Determination of energy barrier for anion transport in NF

In order to calculate the activation energy for Cl^- and NO_3^- passage through the membrane, the solute flux (J_{solute}) was first calculated at four different temperatures of 25, 30, 35, and 40 °C using

$$J_{solute} = J_w C_p \tag{1}$$

where J_w is the water flux through the membrane (L m^{-2} h^{-1}) and C_p is the permeate anion concentration (mmol L^{-1}). The activation energy, E_a, was then calculated from the linearized form of the Arrhenius equation:

$$J_{solute} = B \exp\left(-\frac{E_a}{RT}\right) \tag{2}$$

$$\ln\left(J_{solute}\right) = \ln(B) - \frac{E_a}{R}\frac{1}{T} \tag{3}$$

where J_{solute} is the solute flux, B is the pre-exponential factor, R is the gas constant, and T is the absolute temperature.

2.4. Surface modification of NF membrane by layer-by-layer self-assembly process

Prior to membrane modification by layer-by-layer (LbL) assembly, the NF270 substrate was soaked in 25% v/v isopropanol solution as described in Section 2.2. The pristine membrane was carefully cut into a suitable size and placed on a handmade, specially designed rectangle holder with the active surface layer facing up and held tightly to expose the effective membrane area.

Four different polyelectrolyte solutions were used for surface modification via LbL assembly (Table 1). First, the aqueous solution of cationic polyelectrolyte was contacted with the active surface of the NF270 substrate for 30 min. The excess cationic polyelectrolyte

Table 1
Polyelectrolyte type, pH, polyelectrolyte concentration and salt concentration (sodium chloride) of the deposition solutions used during LbL assembly. The pH of the deposition solution was not adjusted. The polyelectrolyte and salt concentration used in this study were reported previously [35–37].

Solution	pH	Polyelectrolyte concentration (M)	Salt concentration (M)
PSS (-)	6.45	0.02	0.5
PAA (-)	3.15	0.02	0.5
PAH (+)	4.65	0.02	0.5
PDADMAC (+)	6.0	0.02	0.5
NaCl (rinsing solution)	5.6	–	0.5

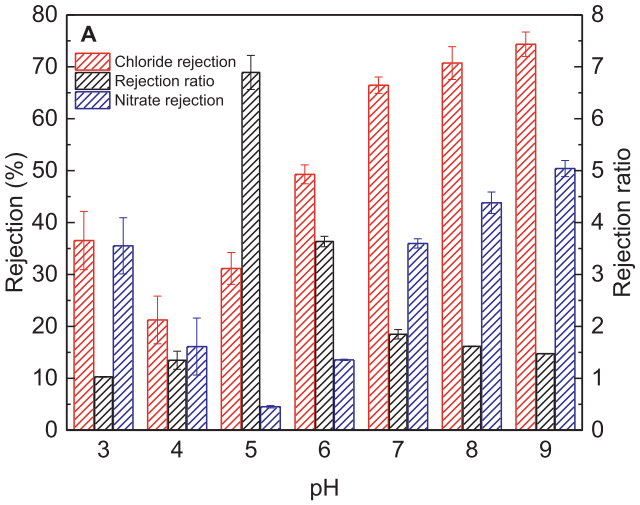

Fig. 1. Anion rejection by the NF270 membrane and rejection ratio (ratio of chloride to nitrate rejection) as a function of feed solution pH. (A) Chloride (Cl^-) rejection, nitrate (NO_3^-) rejection, and Cl^- to NO_3^- rejection ratio for a mixed solution of 4 mM NaCl and 4 mM $NaNO_3$. (B) Cl^- and NO_3^- rejection for a mixed solution of 4 mM NaCl and 4 mM $NaNO_3$. (C) Cl^- and NO_3^- rejection for separate solutions of 4 mM NaCl or 4 mM $NaNO_3$. Experimental conditions during the NF experiments: applied pressure of 3.45 bar (50 psi), initial water flux of 85 L m^{-2} h^{-1}, cross flow velocity of 21.4 cm/s, and temperature of 25 °C.

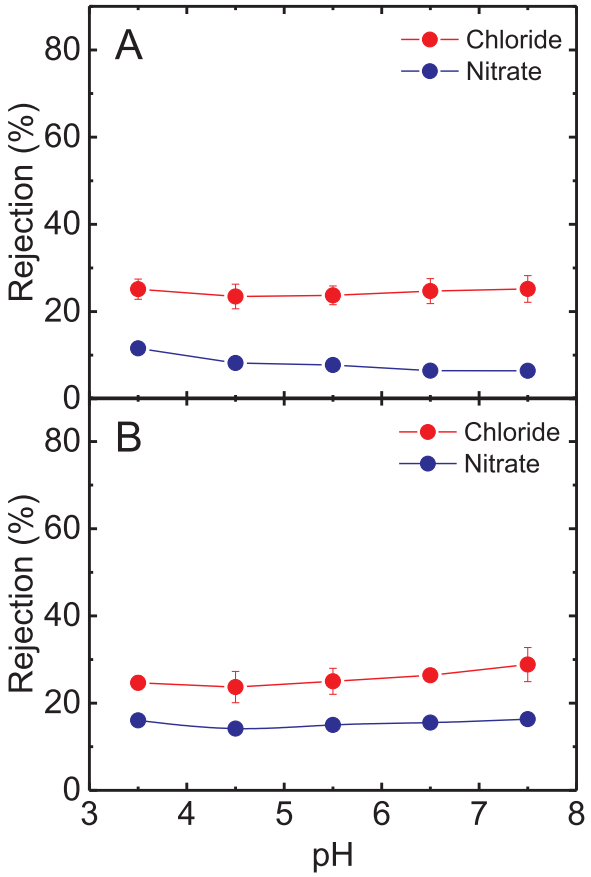

Fig. 2. Anion rejection obtained with the cellulose acetate NF membrane (CK) as a function of feed solution pH. (A) Chloride (Cl^-) and nitrate (NO_3^-) rejection for a mixed solution of 4 mM NaCl and 4 mM $NaNO_3$. (B) Cl^- and NO_3^- rejection for separate solutions of 4 mM NaCl or 4 mM $NaNO_3$. Experimental conditions during the NF experiments: applied pressure of 4.8 bar (70 psi), initial water flux of 25 L m^{-2} h^{-1}, cross flow velocity of 21.4 cm/s, and temperature of 25 °C.

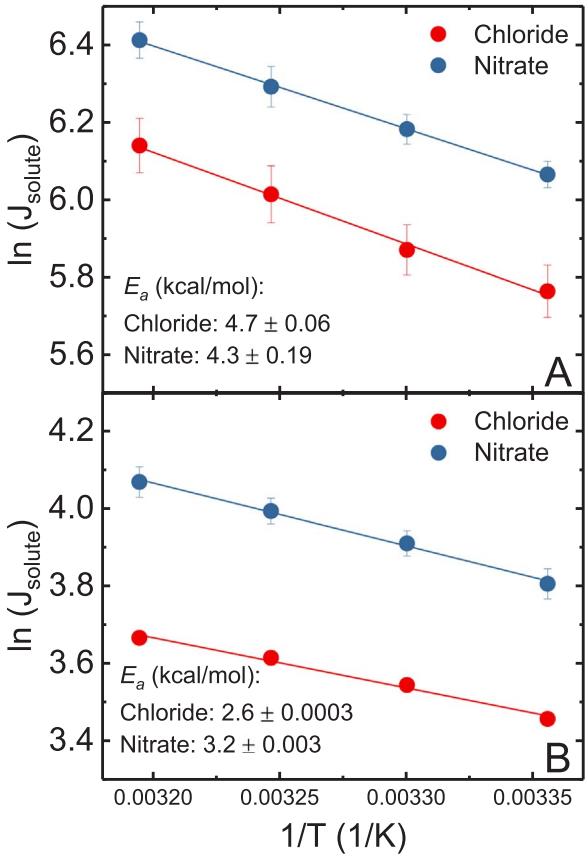

Fig. 3. Activation energy for nitrate and chloride transport through (A) NF270 polyamide NF membrane and (B) CK cellulose acetate NF membrane. Activation energies were determined from the slopes of the plots according to Eq. (3). Anion flux (J_{solute}) expressed in mmol m^{-2} h^{-1} was determined from NF filtration experiments with 4 mM NaCl or $NaNO_3$ at feed solution pH of 5.5 and 5.5 bar (80 psi) applied pressure at different temperatures of 25 °C, 30 °C, 35 °C, and 40 °C. The crossflow velocity for all experiments was fixed at 21.4 cm/s.

solution on the substrate was rinsed by gently contacting the substrate surface with NaCl solution for 10 min (the rinsing stage repeated three times). Next, the anionic polyelectrolyte solution was contacted with the cationic polyelectrolyte-loaded NF270 substrate for 30 min to obtain electrostatic attraction between cationic and anionic polyelectrolyte molecules. Last, the excess anionic polyelectrolyte solution was rinsed by immersing the membrane surface in NaCl solution for 10 min (the rinsing stage repeated three times). After this stage, the first electrostatically assembled bilayer was produced. Multiple bilayers were prepared by repeating the steps mentioned above. After modification, the membrane was immersed in 85% glycerol solution for 4 h and then kept on a dry plate until use. The surface zeta potential of the pristine and modified membranes was determined from streaming potential measurements (EKA Electro Kinetic Analyzer, Anton Paar) as described elsewhere [34].

Table 2
pKa values of the polyelectrolytes used: strong positive (PDADMAC), weak positive (PAH), strong negative (PSS), and weak negative (PAA) polyelectrolytes [42].

Polyelectrolyte	pKa
PSS (-)	1.2–1.5
PAA (-)	4.8–6.8
PAH (+)	8.6–10.3
PDADMAC (+)	N/A

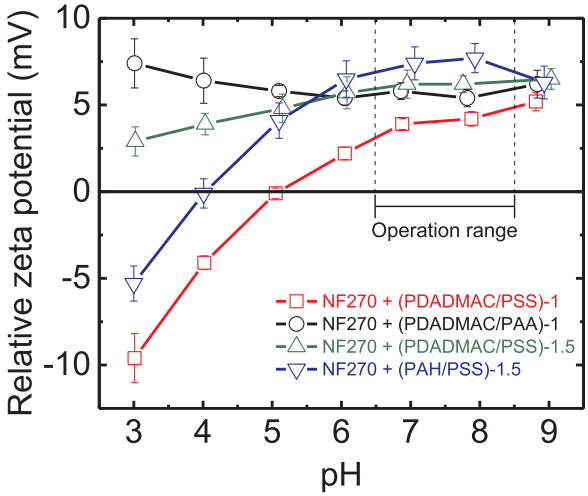

Fig. 4. Relative zeta potential as a function of feed solution pH for different types of polyelectrolyte used to modify the pristine NF270 membrane. The relative zeta potential is defined as the zeta potential of the modified membrane minus the zeta potential of the pristine membrane. The script '1' indicates one bilayer with negative capping. The script '1.5' indicates one and a half bilayers with positive capping. The zeta potential measurement was performed at 25 °C and with a 1 mM KCl solution as the background electrolyte.

3. Results and discussion

3.1. Effect of NF membrane charge on chloride and nitrate rejection

3.1.1. Rejection as a function of feed solution pH with a charged polyamide NF membrane

The first set of experiments was designed to investigate the effect of membrane surface charge on Cl^- and NO_3^- rejection and the Cl^- to NO_3^- rejection ratio using the NF270 membrane (Fig. 1). The NF270 membrane is prepared by interfacial polymerization reaction of a monomeric polyamine with a polyfunctional acyl chloride, resulting in a thin active layer with carboxyl and amine functional groups [38]. We varied the membrane surface charge by adjusting the pH of the feed solution in the range of 3–9.

Fig. 1a presents the pH dependence of the anion rejection and the rejection ratio, revealing a minimum for the rejection of the two anions and a maximum for the Cl^- to NO_3^- rejection ratio at pH 4–5. For symmetrical 1:1 electrolytes, like the NaCl and $NaNO_3$ used in this study, the minimum rejection is achieved near the isoelectric pH [6], indicating that the isoelectric pH of the NF270 membrane is between pH 4 and 5, as was shown previously [39]. The maximum Cl^- to NO_3^- rejection ratio is observed at pH 5, where the membrane is slightly negatively charged. The Cl^- to NO_3^- rejection ratio decreases with an increase in membrane charge for both directions (positive and negative), but it remains above 1 in the negatively charged range (pH > 5). In the positively charged range (pH < 4), the rejection ratio approaches a value close to 1, suggesting that the cation (Na^+) dictates the rejection almost independently of the anion type.

The occurrence of minimum rejection of Cl^- at lower pH than NO_3^- (Fig. 1b) creates a horizontal shift between the rejection curves of the two anions (i.e., the NO_3^- curve is shifted to the right). It was shown earlier that different salts can present different minimum rejection pH for the same membrane due to the nature of the salt [6]. Here, this horizontal shift can be explained by the lower negative ionic charge density of NO_3^- due to its higher ionic volume compared to Cl^- as suggested previously [14,15,21]. Therefore, the repulsion of NO_3^- by the negatively charged membrane starts at higher pH where the negative charge on the membrane surface is higher. The horizontal shift, promoted by a charge-exclusion mechanism, results in a maximum rejection ratio near pH 5 and leads to higher Cl^- rejection than NO_3^- when the membrane is negatively charged (i.e., feed pH > 5), but not when it is positively charged (i.e., feed pH < 4). This set of results indicates that Cl^- rejection is greater than NO_3^- rejection when the membrane is negatively charged due to the Donnan (charge)-exclusion mechanism.

Fig. 1b and c show a higher difference between Cl^- and NO_3^- rejection for the mixed salt solution than for the separate salt solutions, which we attribute to the counter-ion effect and co-ion competition. In the mixed salt solution with the double concentration (8 mM) of Na^+, more Na^+ ions permeate through the membrane, resulting in higher permeation of NO_3^- (the less rejected anion) through the membrane to maintain electroneutrality of the solutions on both sides of the membrane.

3.1.2. Rejection as a function of feed solution pH with an uncharged cellulose acetate NF membrane

A second set of experiments was performed in order to evaluate the effect of pH on Cl^- and NO_3^- rejection using an uncharged cellulose acetate membrane (Fig. 2). Cellulose acetate membranes are prepared via phase inversion and contain no charged functional groups [40]. We varied the feed solution pH over a narrower range (pH 3.5–7.5) to avoid hydrolysis of the cellulose acetate membrane [41].

Fig. 2 shows almost constant rejection for both anions at different feed solution pH values, with higher rejection of Cl^- than NO_3^-. This set of results with an uncharged membrane supports the idea that higher Cl^- than NO_3^- rejection in NF membranes can be also attributed to a size-exclusion mechanism. In general, the relatively low rejection obtained for both anions is attributed to the absence of the Donnan-exclusion mechanism with the cellulose acetate membrane and the "loose" structure of the membrane. The stable rejection at different pH values with an uncharged membrane also suggests that the hydration radius of the anions was maintained stable at different pH and did not affect the observed rejection. This observation supports the results in Section 3.1.1 by showing that the differences in anion rejection with the NF270 membrane at different pH values were due to the change in membrane charge, rather than a difference in the hydrated radius of the anions. As shown earlier for the NF270 membrane (Fig. 1), higher difference between the rejections of the two anions was observed for the mixed salt solution (Fig. 2a) due to the earlier discussed counter-ion effect.

The results in Sections 3.1 and 3.2 suggest that both Donnan (charge)- and size-exclusion mechanisms promote higher Cl^- rejection than NO_3^- rejection in NF membranes. Therefore, the maximum Cl^- to NO_3^- rejection ratio observed with the NF270 membrane at pH 5 (Fig. 1a) can be attributed to the coupling of both mechanisms at this pH.

3.2. Activation energies for chloride and nitrate passage through a charged and uncharged NF membrane

Following the investigation of the effect of membrane charge on Cl^- and NO_3^- rejection, we evaluated the activation energy for the passage of the two anions through the charged (NF270) and uncharged (CK) NF membranes using the linearized form of the Arrhenius equation (Eq. 3). The membrane solute (i.e., Cl^- or NO_3^-) flux (J_{solute}) was measured at different feed solution temperatures in the range of 25–40 °C. The data

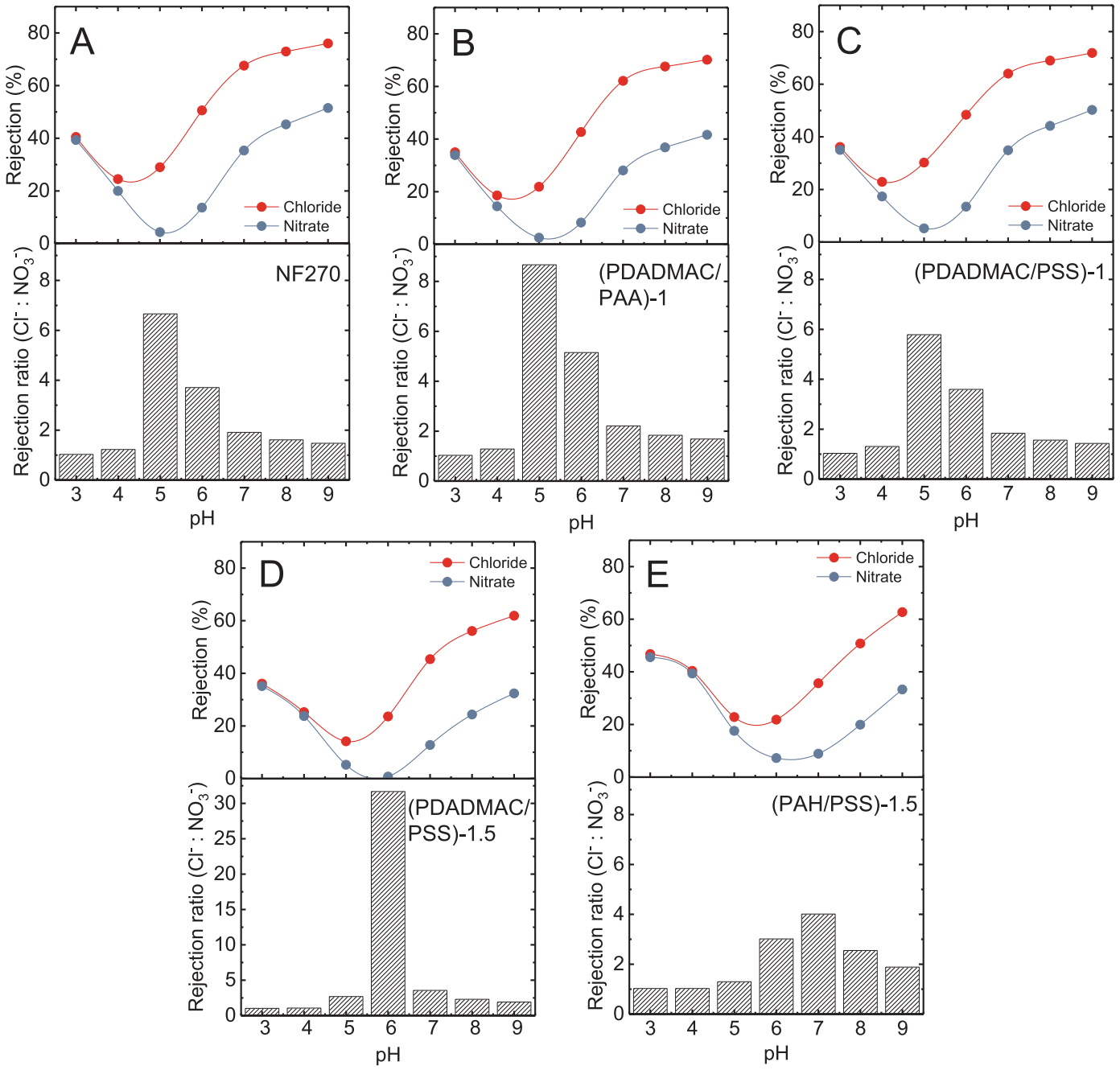

Fig. 5. Anion rejection and rejection ratio (ratio of chloride to nitrate rejection) as a function of feed solution pH. (A) Pristine NF270, initial flux of 80 L m^{-2} h^{-1}. (B) Pristine NF270 + (PDADMAC/PAA) − 1, initial flux of 80 L m^{-2} h^{-1}. (C) Pristine NF270 + (PDADMAC/PSS) − 1, initial flux of 70 L m^{-2} h^{-1}. (D) Pristine NF270 + (PDADMAC/PSS) − 1.5, initial flux of 70 L m^{-2} h^{-1}. (E) Pristine NF270 + (PAH/PSS) − 1.5, initial flux of 50 L m^{-2} h^{-1}. The script '1' indicates one bilayer with negative capping; the script '1.5' indicates one and a half bilayers with positive capping. Experimental conditions during the NF experiments: applied pressure of 3.45 bar (50 psi), cross flow velocity of 21.4 cm/s, and temperature of 25 °C.

were plotted as $ln\,(J_{solute})$ versus $1/T$ to obtain the activation energy from the slope of the curve (Fig. 3).

For both membranes, NO_3^- flux through the membrane was higher than Cl^- flux at the temperature range tested (25–40 °C). For the uncharged membrane (Fig. 3b), a higher activation energy was calculated for NO_3^- than for Cl^-, indicating that the passage of the NO_3^- anion through the membrane is more affected by the temperature than the Cl^- anion. Assuming size exclusion is the main mechanism for the uncharged membrane, the higher flux difference between the two anions at higher temperatures (i.e., the lines of the two anions get further from each other) indicates that at higher temperatures the difference between the hydrated radii of Cl^- and NO_3^- anions approaching the membrane becomes larger. The last observation can be explained by the higher degree of dehydration of the NO_3^- anion compared to Cl^- at higher temperatures due to its lower hydration energy [28,29]. The higher activation energy calculated for NO_3^- compared to Cl^- can also be attributed to other steric effects due to the different geomtrical structure of the anions. As the NO_3^- anion is planar and the Cl^- anion is spherical, the former may need to be in a specific orientation to enter the pore.

The higher activation energy of NO_3^- compared to Cl^- for the uncharged membrane also suggests that statistically, at a given temperature, there are more Cl^- anions than NO_3^- anions that possess sufficient energy to enter into the membrane pore. However, the pre-exponential factor B of NO_3^- is higher, dictating higher NO_3^- flux than Cl^- flux and indicating that at infinite temperature (i.e., the intercept with the

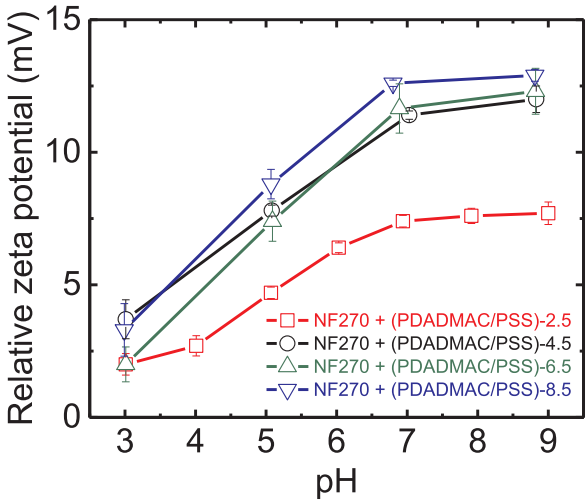

Fig. 6. Relative zeta potential as a function of feed solution pH for varying number of (PDADMAC/PSS) bilayers modification on a pristine NF270 membrane. The relative zeta potential is defined as the zeta potential of the modified membrane minus the zeta potential of the pristine membrane. The script 'x.5' indicates a half bilayer with positive capping. The zeta potential measurement was performed at 25 °C and with a 1 mM KCl solution as the background electrolyte.

vertical axis when *1/T* approaches zero), where the passage of the anions is not limited by any energy barrier, NO_3^- flux is higher. This behavior can be attributed to the more compact form of NO_3^- within the pore due to the higher degree of dehydration compared to Cl^-, allowing the NO_3^- anion to cross the membrane faster.

The measured activation energy is higher for the charged NF270 membrane (Fig. 3a) compared to the uncharged CK membrane (Fig. 3b). This observation is attributed to the different pore size of the two membranes and the existence of two rejection mechanisms with the NF270 membrane, Donnan (charge)-exclusion and size (steric)-exclusion. Moreover, the addition of the Donnan-exclusion mechanism for the NF270 membrane results in a higher activation energy of Cl^- than NO_3^-, suggesting that the Cl^- anion needs more energy to resist the electric repulsion created by the negatively charged membrane. This suggestion corroborates with our previous discussion postulating that Cl^- has higher ionic charge density than NO_3^- due to its smaller volume.

3.3. Controlling the chloride to nitrate rejection ratio via layer-by-layer (LbL) membrane surface charge modification

The results in Sections 3.1 and 3.2 suggest that higher Cl^- than NO_3^- rejection in NF can be attributed to both size (steric)- and Donnan (charge)-exclusion mechanisms due to the different degree of dehydration and different charge density of the two anions, respectively. Additionally, it was shown that the highest Cl^- to NO_3^- rejection ratio with the NF270 membrane is obtained by the coupling of size- and Donnan-exclusion mechanisms at low negative charge near the isoelectric pH (Fig. 1a). Based on this insight, we modified the membrane charge via LbL polyelectrolyte self-assembly to further support our proposed mechanism for the highest Cl^- to NO_3^- rejection ratio near the isoelectric pH and to provide insights for membrane fabrication to control nitrate passage in NF. For NF membranes, which have lower salt rejection compared to RO membranes, the Cl^- to NO_3^- rejection ratio provides a good indicator for the capability of the NF membrane to separate Cl^- and NO_3^- anions [20].

3.3.1. Effect of capping polyelectrolyte type on NF membrane rejection ratio

Four different capping polyelectrolytes with different charge and pKa values were used to control the surface charge of the NF270 membrane (Table 2). The counter polyelectrolyte layer (i.e., the layer with opposite charge to the capping layer) was PDADMAC (for negative capping) and PSS (for positive capping).

At this stage, a minimal number of bilayers (1 for negative and 1.5 for positive capping) was applied in order to evaluate the effect of polyelectrolyte type on membrane surface charge. The surface charge of the modified membranes was characterized by the relative zeta potential which is defined as the difference between the zeta potential of the modified membrane and the zeta potential of the pristine NF270 membrane at different pH values (Fig. 4).

Fig. 4 shows that all polyelectrolyte modifications resulted in more positive membrane surface charge at pH 6.5–8.5 due to the strong negative surface charge of the pristine NF270 membrane. Following membrane surface charge characterization, the modified membranes were tested for Cl^- and NO_3^- rejection at different pH values (Fig. 5).

Fig. 5 shows that for the membranes with negative capping (Fig. 5b and c), the isoelectric pH remained at 5 as for the pristine membrane (Fig. 5a). For the membranes with positive capping, the isoelectric pH shifted to pH 6 (Fig. 5d) and pH 7 (Fig. 5e). The highest Cl^- to NO_3^- rejection ratio was always observed at slightly above the isoelectric pH (i.e., the pH with the lowest rejections), supporting our earlier idea that the maximum rejection ratio is obtained by coupling of both size-exclusion and Donnan-exclusion mechanisms. The very high rejection ratio for the modification with (PDADMAC/PSS) − 1.5 at pH 6 (Fig. 5d) is a result of the extremely low NO_3^- rejection (< 1%) observed in this case. The different values of the maximum rejection ratio observed with the different membranes can be related to the proximity of the feed pH tested to the actual pH in which the maximum rejection ratio is obtained. As discussed in Section 3.1, Fig. 5 shows that at positive membrane charge, the rejection is dictated by the the Na^+ cation, independently of the anion type.

Both membranes with positive capping presented higher isoelectric pH (Fig. 5d and e). However, we decided to use the (PDADMAC/PSS) − 1.5 membrane (Fig. 5d) in our further study to explore the effect of the bilayers number on the rejection ratio. Besides its very high maximum rejection ratio (~32), our rationale suggests that addition of more bilayers can lead to further increase of the isoelectric pH due to the more positive zeta potential of the membrane [37], thereby allowing the fabrication of NF membranes with high Cl^- to NO_3^- rejection ratio at the typical pH of natural waters.

3.3.2. Effect of the number of polyelectrolyte layers on NF membrane rejection ratio

Fig. 6 presents the relative zeta potential of (PDADMAC/PSS) membranes with different number of bilayers compared to the zeta potential of the pristine NF270 membrane as a function of feed solution pH. In general, higher (more positive) membrane charge was observed with a higher bilayers number. This observation can be attributed to the more effective coverage of the negative charge of the pristine membrane with higher number of bilayers. The gradual coverage of the pristine membrane surface charge can also explain the smaller change in zeta potential with addition of more bilayers.

Following membrane surface charge characterization, the modified (PDADMAC/PSS) membranes containing different number of bilayers were tested for Cl^- and NO_3^- rejection at different feed solution pH. Fig. 7 shows that the isoelectric pH shifted up with a higher number of bilayers due to the increase in membrane charge (Fig. 6). As a result, the highest Cl^- to NO_3^- rejection ratio was also obtained at higher pH. In general, with a higher number of bilayers, the maximum rejection ratio near the isoelectric pH decreases due to the increase in NO_3^- rejection at this point (except for the pristine membrane, Fig. 7a). A higher Cl^- to NO_3^- rejection ratio was always obtained at the negative side (pH > isoelectric pH) than at the positive side (pH < isoelectric pH), as observed previously.

All modified membranes showed a higher Cl^- to NO_3^- rejection ratio (2.5–5) than the pristine NF270 membrane (< 2) at pH 7–9 due to the more positive membrane surface charge and the higher proximity to the isoelectric pH in this pH range. Increasing the number of bilayers,

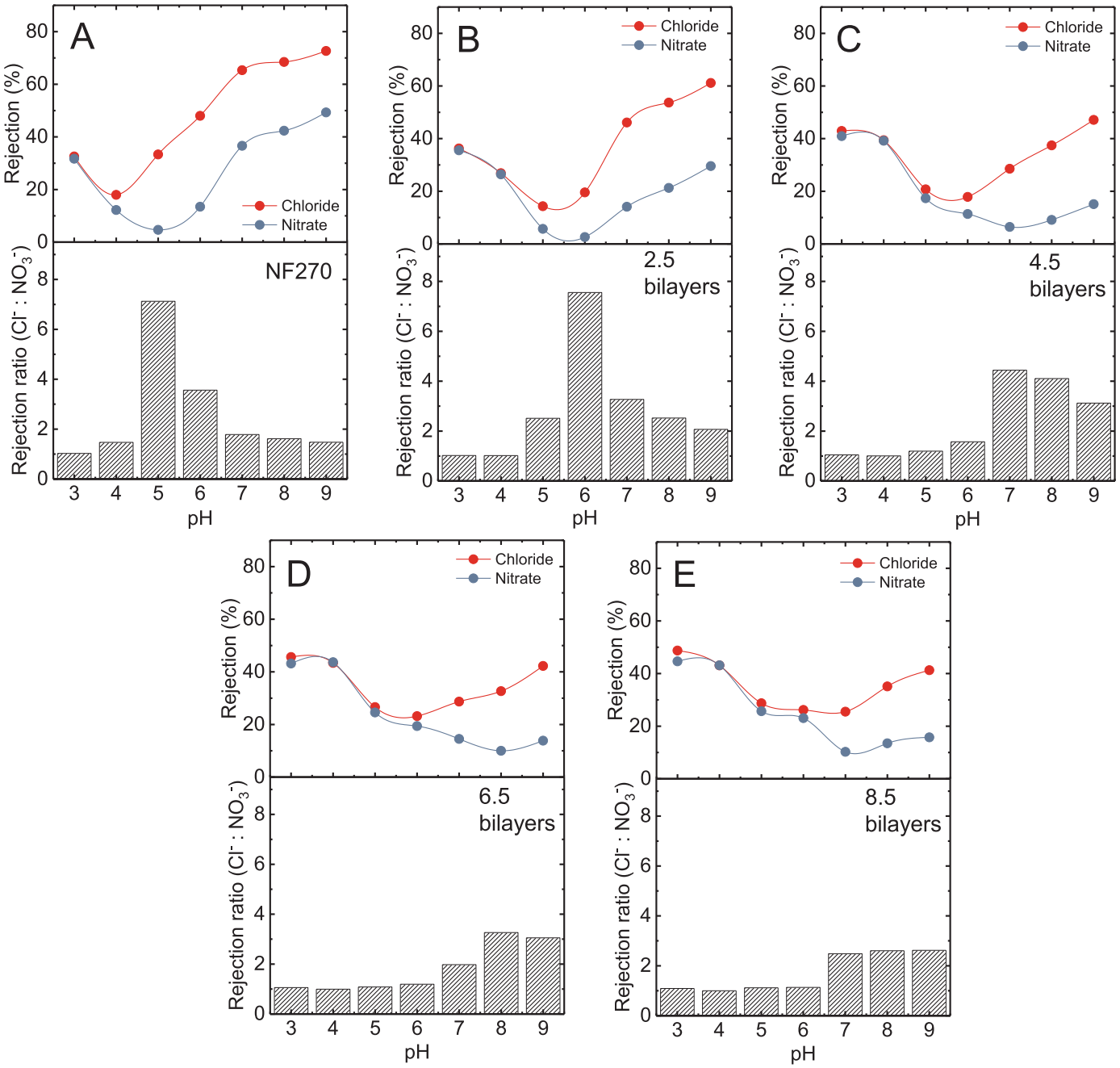

Fig. 7. Anion rejection and rejection ratio (ratio of chloride to nitrate rejection) as a function of feed solution pH. (A) Pristine NF270. (B) Pristine NF270 + (PDADMAC/PSS)−2.5. (C) Pristine NF270 + (PDADMAC/PSS)−4.5. (D) Pristine NF270 + (PDADMAC/PSS)−6.5. (E) Pristine NF270 + (PDADMAC/PSS)−8.5. The subscript 'x.5' indicates a half bilayer with positive capping. Experimental conditions during the NF experiments: applied pressure of 3.45 bar (50 psi), cross flow velocity of 21.4 cm/s, and temperature of 25 °C.

however, also decreases the membrane pure water permeability (Fig. 8) and the maximum rejection ratio (Fig. 7) due to the increase in membrane thickness and NO_3^- rejection, respectively. For the membranes tested in our study, the optimal number of bilayers providing high Cl^- to NO_3^- rejection ratio at neutral pH while still providing reasonable water permeability lies between 1.5 and 4.5 (PDADMAC/PSS) bilayers.

4. Conclusion

The reasons for the higher Cl^- than NO_3^- rejection by NF membranes were investigated, using polyamide-based (NF270) and cellulose acetate-based (CK) NF membranes. By systematically controlling the pH of separate and mixed aqueous NaCl and $NaNO_3$ feed solutions, followed by calculation of the activation energy for Cl^- and NO_3^- passage through the membranes, it was shown that both size (steric)-exclusion and Donnan (charge)-exclusion mechanisms promote higher Cl^- than NO_3^- rejection in NF. The NO_3^- anion has lower hydration energy than Cl^- and therefore can undergo a higher degree of dehydration and cross the membrane pores faster. The Cl^- anion, with its lower ionic volume, has higher ionic charge density compared to NO_3^- and therefore is repelled more than NO_3^- by a negatively charge membrane. Coupling of both size- and charge-exclusion mechanisms results in a maximum Cl^- to NO_3^- rejection ratio at low negative membrane charge near the isoelectric pH value of the polyamide membrane. We showed the potential for increasing NF membrane selectivity to NO_3^- passage over Cl^- at near neutral feed solution pH by shifting the isoelectric pH of the membrane from pH 4–5 to pH 6–9 via LbL polyelectrolyte self-assembly.

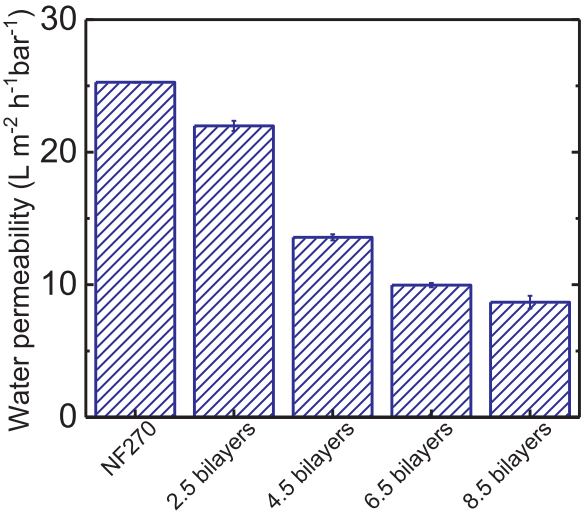

Fig. 8. Pure water permeability of pristine NF270 and modified membranes with varying number of (PDADMAC/PSS) bilayers determined at an applied pressure of 3.45 bar (50 psi), feed solution pH of 5.5, crossflow velocity of 21.4 cm/s, and a temperature of 25 °C.

Acknowledgements

This research was made possible by the postdoctoral fellowship (to Dr. Razi Epsztein) provided from the United States–Israel Binational Agricultural Research and Development Fund BARD, Fellowship number FI-549-2016. We also acknowledge the Scientific and Technological Research Council of Turkey, the Department of Science Fellowships and Grant Programs (1059B191501137) for financially supporting Dr. Nadir Dizge.

References

[1] B. Van der Bruggen, C. Vandecasteele, Removal of pollutants from surface water and groundwater by nanofiltration: overview of possible applications in the drinking water industry, Environ. Pollut. 122 (2003) 435–445.
[2] N. Hilal, H. Al-Zoubi, N.A. Darwish, A.W. Mohammad, M. Abu Arabi, A comprehensive review of nanofiltration membranes: treatment, pretreatment, modelling, and atomic force microscopy, Desalination 170 (2004) 281–308, http://dx.doi.org/10.1016/j.desal.2004.01.007.
[3] A.W. Mohammad, Y.H. Teow, W.L. Ang, Y.T. Chung, D.L. Oatley-Radcliffe, N. Hilal, Nanofiltration membranes review: recent advances and future prospects, Desalination 356 (2015) 226–254, http://dx.doi.org/10.1016/j.desal.2014.10.043.
[4] D. Zhou, L. Zhu, Y. Fu, M. Zhu, L. Xue, Development of lower cost seawater desalination processes using nanofiltration technologies – a review, Desalination 376 (2015) 109–116, http://dx.doi.org/10.1016/j.desal.2015.08.020.
[5] B. Van der Bruggen, M. Mänttäri, M. Nyström, Drawbacks of applying nanofiltration and how to avoid them: a review, Sep. Purif. Technol. 63 (2008) 251–263, http://dx.doi.org/10.1016/j.seppur.2008.05.010.
[6] J. Luo, Y. Wan, Effects of pH and salt on nanofiltration-a critical review, J. Membr. Sci. 438 (2013) 18–28, http://dx.doi.org/10.1016/j.memsci.2013.03.029.
[7] M. Lunau, M. Voss, M. Erickson, C. Dziallas, K. Casciotti, H. Ducklow, Excess nitrate loads to coastal waters reduces nitrate removal efficiency: mechanism and implications for coastal eutrophication, Environ. Microbiol. 15 (2013) 1492–1504, http://dx.doi.org/10.1111/j.1462-2920.2012.02773.x.
[8] D.M. Manassaram, L.C. Backer, D.M. Moll, A review of nitrates in drinking water: maternal exposure and adverse reproductive and developmental outcomes, Environ. Health Perspect. 114 (2006) 320–327, http://dx.doi.org/10.1289/ehp.8407.
[9] M.A. Shannon, P.W. Bohn, M. Elimelech, J.G. Georgiadis, B.J. Marinas, A.M. Mayes, Science and technology for water purification in the coming decades, Nature 452 (2008) 301–310, http://dx.doi.org/10.1038/nature06599.
[10] J.R. Werber, A. Deshmukh, M. Elimelech, The critical need for increased selectivity, not increased water permeability, for desalination membranes, Environ. Sci. Technol. Lett. 3 (2016) 112–120, http://dx.doi.org/10.1021/acs.estlett.6b00050.
[11] U. Kafkafi, Effects of chlorides in effluents used for irrigation on the irrigated crops, Isr. J. Planet. Sci. 59 (2011) 2–4.
[12] A.E. Childress, M. Elimelech, Relating nanofiltration membrane performance to membrane charge (electrokinetic) characteristics, Environ. Sci. Technol. 34 (2000) 3710–3716, http://dx.doi.org/10.1021/es0008620.
[13] A.G. Volkov, S. Paula, D.W. Deamer, Two mechanisms of permeation of small neutral molecules and hydrated ions across phospholipid bilayers, Bioelectrochem. Bioenerg. 42 (1997) 153–160, http://dx.doi.org/10.1016/S0302-4598(96)05097-0.
[14] M.A. Amouha, G.R.N. Bidhendi, B. Hooshyari, Nanofiltration Efficiency in Nitrate Removal from Groundwater: A Semi-Industrial Case Study, in: Proceedings of the 2nd International Conference Environ. Eng. Appl., Singapore, 2011.
[15] D.X. Wang, M. Su, Z.Y. Yu, X.L. Wang, M. Ando, T. Shintani, Separation performance of a nanofiltration membrane influenced by species and concentration of ions, Desalination 175 (2005) 219–225.
[16] C.K. Diawara, L. Paugam, M. Pontié, J.P. Schlumpf, P. Jaouen, F. Quéméneur, Influence of chloride, nitrate, and sulphate on the removal of fluoride ions by using nanofiltration membranes, Sep. Sci. Technol. 40 (2005) 3339–3347, http://dx.doi.org/10.1080/01496390500423706.
[17] K. Hayrynena, E. Pongracza, V. Vaisanena, N. Papa, M. Manttaric, J. Langwaldtd, R.L. Keiskia, Concentration of ammonium and nitrate from mine water by reverse osmosis and nanofiltration, Desalination 240 (2009) 280–289.
[18] A. Santafé-Moros, J.M. Gozálvez-Zafrilla, J. Lora-García, Nitrate removal from ternary ionic solutions by a tight nanofiltration membrane, Desalination 204 (2007) 63–71.
[19] F. Garcia, D. Ciceron, A. Saboni, S. Alexandrova, Nitrate ions elimination from drinking water by nanofiltration: membrane choice, Sep. Purif. Technol. 52 (2006) 196–200.
[20] R. Epsztein, O. Nir, O. Lahav, M. Green, Selective nitrate removal from groundwater using a hybrid nanofiltration–reverse osmosis filtration scheme, Chem. Eng. J. 279 (2015) 372–378, http://dx.doi.org/10.1016/j.cej.2015.05.010.
[21] M. Thanuttamavong, K. Yamamoto, J. Ik Oh, K. Ho Choo, S. June Choi, Rejection characteristics of organic and inorganic pollutants by ultra low-pressure nanofiltration of surface water for drinking water treatment, Desalination 145 (2002) 257–264, http://dx.doi.org/10.1016/S0011-9164(02)00420-4.
[22] L. Paugam, C.K. Diawara, J.P. Schlumpf, P. Jaouen, F. Quéméneur, Transfer of monovalent anions and nitrates especially through nanofiltration membranes in brackish water conditions, Sep. Purif. Technol. 40 (2004) 237–242, http://dx.doi.org/10.1016/j.seppur.2004.02.012.
[23] L. Paugam, S. Taha, G. Dorange, P. Jaouen, F. Quéméneur, Mechanism of nitrate ions transfer in nanofiltration depending on pressure, pH, concentration and medium composition, J. Memb. Sci. 231 (2004) 37–46, http://dx.doi.org/10.1016/j.memsci.2003.11.003.
[24] L. Li, J. Dong, T.M. Nenoff, Transport of water and alkali metal ions through MFI zeolite membranes during reverse osmosis, Sep. Purif. Technol. 53 (2007) 42–48, http://dx.doi.org/10.1016/j.seppur.2006.06.012.
[25] B. Tansel, J. Sager, T. Rector, J. Garland, R.F. Strayer, L. Levine, M. Roberts, M. Hummerick, J. Bauer, Significance of hydrated radius and hydration shells on ionic permeability during nanofiltration in dead end and cross flow modes, Sep. Purif. Technol 51 (2006), pp. 40–47, http://dx.doi.org/10.1016/j.seppur.2005.12.020.
[26] B. Tansel, Significance of thermodynamic and physical characteristics on permeation of ions during membrane separation: hydrated radius, hydration free energy and viscous effects, Sep. Purif. Technol. 86 (2012) 119–126, http://dx.doi.org/10.1016/j.seppur.2011.10.033.
[27] S.M.S. Ghiu, R.P. Carnahan, M. Barger, Mass transfer in RO TFC membranes - dependence on the salt physical and thermodynamic parameters 157 (2003) 385–393.
[28] L.A. Richards, A.I. Schafer, B.S. Richards, B. Corry, Quantifying barriers to monovalent anion transport in narrow non-polar pores, Phys. Chem. Chem. Phys. 14 (2012) 11633–11638, http://dx.doi.org/10.1039/c2cp41641g.
[29] L.A. Richards, B.S. Richards, B. Corry, A.I. Schafer, Experimental Energy Barriers to Anions Transporting through Nano fi ltration Membranes (2013).
[30] K. Linde, A.S. Jönsson, Nanofiltration of salt solutions and landfill leachate, Desalination 103 (1995) 223–232, http://dx.doi.org/10.1016/0011-9164(95)00075-5.
[31] S. Choi, Z. Yun, S. Hong, K. Ahn, The effect of co-existing ions and surface characteristics of nanomembranes of the removal of nitrate and fluoride, Desalination 133 (2001) 53–64, http://dx.doi.org/10.1016/S0011-9164(01)00082-0.
[32] C. Ratanatamskul, K. Yamamoto, T. Urase, S. Ohgaki, Effect of operating conditions on rejection of anionic pollutants in the water environment by nanofiltration especially in very low pressure range, Water Sci. Technol. 34 (1996) 149–156, http://dx.doi.org/10.1016/S0273-1223(96)00798-6.
[33] C. Ratanatamskul, T. Urase, K. Yamamoto, Description of behavior in rejection of pollutants in ultra low pressure nanofiltration, Water Sci. Technol. 38 (1998) 453–462, http://dx.doi.org/10.1016/S0273-1223(98)00545-9.
[34] Y.C. Chiang, Y.Z. Hsub, R.C. Ruaan, C.J. Chuang, K.L. Tung, Nanofiltration membranes synthesized from hyperbranched polyethyleneimine, J. Membr. Sci. 326 (2009) 19–26, http://dx.doi.org/10.1016/j.memsci.2008.09.021.
[35] S.U. Hong, R. Malaisamy, M.L. Bruening, Optimization of flux and selectivity in Cl-/SO42- separations with multilayer polyelectrolyte membranes, J. Membr. Sci. 283 (2006) 366–372, http://dx.doi.org/10.1016/j.memsci.2006.07.007.
[36] L. Ouyang, R. Malaisamy, M.L. Bruening, Multilayer polyelectrolyte films as nanofiltration membranes for separating monovalent and divalent cations, J. Membr. Sci. 310 (2008) 76–84, http://dx.doi.org/10.1016/j.memsci.2007.10.031.
[37] R. Malaisamy, A. Talla-Nwafo, K.L. Jones, Polyelectrolyte modification of nanofiltration membrane for selective removal of monovalent anions, Sep. Purif. Technol. 77 (2011) 367–374, http://dx.doi.org/10.1016/j.seppur.2011.01.005.
[38] A.E. Childress, M. Elimelech, Effect of solution chemistry on the surface charge of polymeric reverse osmosis and nanofiltration membranes, J. Membr. Sci. 119 (1996) 253–268, http://dx.doi.org/10.1016/0376-7388(96)00127-5.
[39] Y.L. Lin, P.C. Chiang, E.E. Chang, Removal of small trihalomethane precursors from aqueous solution by nanofiltration, J. Hazard. Mater. 146 (2007) 20–29, http://dx.doi.org/10.1016/j.jhazmat.2006.11.050.
[40] B.S. Lalia, V. Kochkodan, R. Hashaikeh, N. Hilal, A review on membrane fabrication: structure, properties and performance relationship, Desalination 326 (2013) 77–95, http://dx.doi.org/10.1016/j.desal.2013.06.016.
[41] S.B. McCray, V.L. Vilker, K. Nobe, Reverse osmosis cellulose acetate membranes. I. Rate of hydrolysis, J. Membr. Sci. 59 (1991) 305–316.
[42] B.N. Dickhaus, R. Priefer, Determination of polyelectrolyte pKa values using surface-to-air tension measurements, Colloids Surf. A Physicochem. Eng. Asp. 488 (2016) 15–19, http://dx.doi.org/10.1016/j.colsurfa.2015.10.015.